Fibrin-fiber architecture influences cell spreading and differentiation

Stéphanie MC Bruekers[1†], Maarten Jaspers[1†], José MA Hendriks[1], Nicholas A Kurniawan[2,3], Gijsje H Koenderink[2], Paul HJ Kouwer[1], Alan E Rowan[1,4]* & Wilhelm TS Huck[1]*

1. Radboud University, Institute for Molecules and Materials, Heyendaalseweg 135, 6525 AJ Nijmegen, The Netherlands

2. FOM Institute AMOLF, Systems Biophysics Department, Science Park 104, 1098 XG Amsterdam, The Netherlands

3. Current address: Eindhoven University of Technology, Department of Biomedical Engineering, P.O. Box 513, 5600 MB Eindhoven, The Netherlands

4. Current address: The University of Queensland, Australian Institute for Bioengineering and Nanotechnology, Brisbane QLD 4072, Australia

[†] These authors contributed equally.

Correspondence to Wilhelm Huck email: w.huck@science.ru.nl or Alan Rowan email: a.rowan@science.ru.nl

Keywords

Fibrin

Fiber architecture

Mesenchymal stem cells

Strain stiffening

Mechanotransduction

Turbidity

Rheology

Differentiation

Hydrogels

Abbreviations and acronyms

ECM	extracellular matrix
hMSC	human mesenchymal stem cell
PIC	polyisocyanopeptide
FBS	fetal bovine serum
LCST	lower critical solution temperature

Abstract

The mechanical and structural properties of the extracellular matrix (ECM) play an important role in regulating cell fate. The natural ECM has a complex fibrillar structure and shows nonlinear mechanical properties, which are both difficult to mimic synthetically. Therefore, systematically testing the influence of ECM properties on cellular behavior is very challenging. In this work we show two different approaches to tune the fibrillar structure and mechanical properties of fibrin hydrogels. Addition of extra thrombin before gelation increases the protein density within the fibrin fibers without significantly altering the mechanical properties of the resulting hydrogel. On the other hand,

by forming a composite hydrogel with a synthetic biomimetic polyisocyanide network the protein density within the fibrin fibers decreases, and the mechanics of the composite material can be tuned by the PIC/fibrin mass ratio. The effect of the changes in gel structure and mechanics on cellular behavior are investigated, by studying human mesenchymal stem cell (hMSC) spreading and differentiation on these gels. We find that the trends observed in cell spreading and differentiation cannot be explained by the bulk mechanics of the gels, but correlate to the density of the fibrin fibers the gels are composed of. These findings strongly suggest that the microscopic properties of individual fibers in fibrous networks play an essential role in determining cell behavior.

Introduction

The adhesion of cells to the extracellular matrix (ECM) has a profound impact on celullar behaviour, influencing cell spreading, migration and differentiation.[1, 2] Precisely how cells sense their environment is still unclear but it is now well-established that the mechanical properties of the ECM play an important role.[3-5] Studies on 2D model substrates, typically polyacrylamide hydrogels, have shown that cells spread more on stiff substrates and tend to differentiate into lineages reflecting the stiffness of the substrate.[3] Hydrogels composed of flexible synthetic polymers, however, do not adequately represent the physical nature of the ECM. The extracellular biopolymer networks in the human body, for example collagen and fibrin, are usually fibrillar and are composed of crosslinked semiflexible fibers. These fibers are formed through bundling of individual filaments, leading to a complex hierarchical structure.[6] This structural design gives these networks unique mechanical properties known as strain stiffening, i.e. their stiffness increases under deformation.[7] The mechanics of these biomaterials are thought to play a fundamental role in their biological function through a process of mechanotransduction.[8-11] In contrast to natural ECM gels, commonly used synthetic hydrogels do not possess such strain-stiffening properties and their stiffness remains constant up to very large strains.[7] In recent studies it has been shown that not only bulk mechanical properties, but also the specific interaction of cells with individual fibers is crucial in tailoring the cellular response.[12]

In our study, we are interested in tailoring the structural properties of the fibers of a biopolymer network and studying how this influences cell behavior. As a model system, we chose fibrin, a plasma protein that has a natural function as a cell scaffold during wound healing and is popular for clinical and bioengineering applications.[13] Here, we show two different approaches for changing both the individual fiber architecture and the bulk gel mechanics of fibrin hydrogels. In the first approach we added extra thrombin to the fibrinogen solution, which results in an increase of the fibrin polymerization rate and changes the architecture of the resulting fibrin fibers. In the second approach we combined fibrin with a second polymer network based on synthetic polyisocyanopeptides (PICs).[14] This synthetic polymer based hydrogel has been shown to exhibit strain-stiffening behavior in the same stress range as many biopolymer gels, including fibrin.[7, 13, 15] This similarity of the mechanical properties prompted us to combine the PICs with fibrin in order to tailor the mechanical properties of the fibrin network within these hybrid hydrogels. We confine our studies on fibrin/PIC hydrogels to planar substrates, as cell spreading and differentiation as a function of the mechanical properties of the substrate have been extensively studied in 2D.

Results

In the present study, three series of fibrin gels were prepared with a fibrin concentration ranging from 1 to 5 mg mL^{-1}. In the first series, fibrin gels were formed by mixing fibrinogen solutions in PBS with an equal volume of cell culture medium (DMEM + 10 % FBS). The thrombin present in the FBS converts fibrinogen into fibrin monomers and initiates their association into a network of fibrils. The second series of fibrin gels were prepared similarly to the first series, but an additional 0.5 U mL^{-1} thrombin was added to increase the rate of gelation. For the third series, fibrin/PIC composite gels were obtained by mixing fibrinogen solutions with 2 mg mL^{-1} solutions of PIC in cell culture medium in the liquid state on ice. Heating this mixture to 37 ˚C leads to the formation of a PIC network due to the LCST nature of this polymer and activation of thrombin. In this way, a fibrin network is formed within the pre-formed PIC network. Confocal microscopy on fluorescently labelled fibrin showed that

the fibrin network structure is significantly altered by the presence of PIC, resulting in a more heterogeneous network of thicker fibrin bundles. In contrast the fibrin and fibrin + thrombin gels are not significantly different (Figure 1A).

The structural differences in the fibrin networks were further analyzed by turbidimetry.[16, 17] This technique provides quantitative information on the diameter and molecular packing density of individual fibers by measuring the scattered light intensity as a function of wavelength.[18] For a suspension of randomly oriented, long and thin cylindrical fibers, the turbidity is a function of the fiber radius r, the mass/length ratio of the fibers μ and the fibrin concentration c (details in experimental section). The fiber diameter is known to be dependent on the fibrin concentration,[19] but several trends among the three series can be observed (Figure 1B). The fiber bundles in normal fibrin gels of 1 to 5 mg mL^{-1} have an average diameter that systematically decreases with fibrin concentration from 240 to 210 nm, consistent with prior work.[20] The presence of PIC resulted in an increase in the bundle diameter: the average diameter ranges from 270 to 230 nm and is larger than for pure fibrin gels at each fibrin concentration examined. The addition of extra thrombin to the fibrinogen solution had little effect on samples of low concentration (1 and 2 mg/ml), but led to thinner bundles than in pure fibrin gels at high fibrin concentration (3 - 5 mg/ml). Under these conditions, the diameter systematically decreased from 250 to 180 nm with increasing fibrin concentration. Based on the measured mass/length ratio of the fiber, the number of protofibrils per fiber N can be extracted from these measurements (Figure 1C). For pure fibrin networks, N increased with fibrin concentration, from 90 protofibrils per fiber at 1 mg/ml fibrin to to 110 at 5 mg/ml fibrin. The addition of extra thrombin had little effect on samples of low concentration, but resulted in a higher N for the high concentration gels. The maximum number of protofibrils per fiber was now 150 at a fibrin concentration of 5 mg mL^{-1}. At the lower fibrin concentrations, thrombin can be assumed not to be the limiting factor in the gelation process and thus the addition of extra thrombin has no effect on the resulting gel structure. Surprisingly, the presence of PIC caused a reduction of N over

the entire fibrin concentration range, with *N* now ranging from 70 to 100. Apparently, the molecular packing density of the fibers is reduced in the presence of PIC.[21]

From the combined information on fiber diameter and the number of protofibrils per fiber, we can calculate the protein mass density within the fibers under the assumption that the fibers have a cylindrical shape (Figure 1D).[17] Since the fibrin fiber diameter is largest in the fibrin/PIC composite networks while the number of protofibrils per fiber is the smallest, these fibers have a much smaller protein density (30 - 60 mg mL^{-1}) than in the case of pure fibrin and fibrin/thrombin networks. For the pure fibrin networks, the density increases from 40 to 80 mg mL^{-1} with increasing fibrin concentration, while for the fibrin/thrombin networks the density increases more strongly, from 40 to 140 mg mL^{-1}.

These results suggest that the presence of the PIC network, which is formed prior to fibrin gelation (Figure S1), leads to fibrin bundles which have intercalating PIC fibers, thus changing the architecture and hence mechanical properties of the fibrin network. A model that can potentially account for these findings is the recent fiber packing structure proposed by Yang[22] and adapted by Yeromonahos[23], which is depicted in Figure 1E. According to this model, the protofibrils are packed in a crystalline lattice, but gaps where protofibrils are missing introduce disorder. Experimental support for this model comes from small angle X-ray scattering measurements, which revealed a fractal-like disordered scattering pattern combined with broad peaks indicating partial order.[23] Given the marked difference in packing density of the fibers formed under different assembly conditions, we expect that the fibers formed in the presence of PIC are more loosely packed and hence more flexible than in pure fibrin gels.[19]

To test whether the differences in network structure affect the mechanics of the fibrin and fibrin/PIC composite hydrogels on the macroscopic scale, we performed shear rheology measurements (Figure 2). Since fibrin and PIC gels individually are both strongly strain-stiffening materials, the stiffness was measured as a function of the applied stress using a pre-stress protocol.[24] The stiffness of these materials is described by the differential modulus $K' = \delta\sigma/\delta\gamma$, where σ and γ are

the stress and strain respectively. For PIC hydrogels, K' shows two distinct regimes: a linear regime where the stiffness is constant and K' equals the plateau modulus G_0 and a nonlinear regime where the stiffness increases with applied stress as $K' \sim \sigma^{3/2}$ (open circles in Figure 2C).[15] This 3/2 exponent is associated to the entropic elasticity of semiflexible polymers.[25, 26] The mechanical response of the fibrin gels is more complex: with increasing shear stress, there is a linear regime, which is followed by a strain-stiffening regime, then a second strain-independent regime, and finally another strain-stiffening regime (Figure 2A). This complex behavior was recently shown to originate from the hierarchical architecture of the fibers.[19] The first stiffening regime is entropic in origin and results from pulling out thermal slack from fiber segments between cross-links, while the second stiffening regime is the result of force-induced changes in the molecular packing structure of the fibers. The first stiffening regime shows a stress-dependence of about $K' \sim \sigma^{0.8}$ whilst the second stiffening regime is expected to eventually reach $K' \sim \sigma^{3/2}$ at very high stress[19] (Figure 2A).

The addition of extra thrombin has little effect on the mechanical response of the fibrin gels (Figure 2C), and the same $K' \sim \sigma^{0.8}$ relationship as observed for normal fibrin gels was found. The addition of thrombin also has little effect on G_0 (Figure 2D) and on the critical stress σ_c, where the fibrin gel starts to stiffen (Figure 2E). The almost identical macroscopic mechanics are somewhat surprising since the addition of thrombin does change the architecture of the fibrin fibers on the microscopic scale (Figure 1). Theoretical models for semi-flexible networks predict that stiffer and more densely packed fibers should lead to stiffer gels with a higher G_0.[26, 27] The fact that no increase in G_0 was observed can only be explained by a transition from a tight to a more loose fiber regime.[20, 28] The addition of thrombin increases the density of the fibrin fibers, but apparently decreases the "coherence" between the protofibrils within the fiber, in analogy to what happens in growing actin bundles.[29]

Interestingly, the fibrin/PIC composite gels show a stiffening response that lies in between the response of the separate fibrin and PIC networks (Figure 2C). When the two components are mixed in a 1:1 mass ratio, the stiffening response is similar to that of the single PIC network with $K' \sim$

$\sigma^{3/2}$. However when the fibrin to PIC ratio is increased to 5:1, the nonlinear stress-response is more similar to that of a pure fibrin network, with $K' \sim \sigma^{0.8}$. This indicates that an applied stress causes deformation of both the fibrin network and the PIC network, which both contribute to the strain-stiffening response of the composite material. The presence of PIC also contributes to G_0 of the composite gels and significantly increases σ_c. The PIC gels have a critical stress of about 3 Pa, which is higher than for fibrin gels due to the much smaller persistence length of the PIC fibers compared to fibrin fibers. This causes the composite gels to be less sensitive to small stresses than pure fibrin gels.

The three different fibrin gels enable us to vary both the bulk mechanics and the fiber architecture of the resulting fibrin networks. Since substrate properties are believed to dictate cell behavior,[30] human mesenchymal stem cell (hMSC) spreading and differentiation on the different gels were studied in two dimensional environments. For cell morphology studies, hMSCs were seeded onto the gels at low cell densities to study cell-matrix interactions and prevent cell-cell signaling. After 24 h incubation, the cells were fixed, actin and nuclear stainings were performed, and the average cell areas were quantified from confocal microscopy images (Figure 3). Cells on fibrin gels were observed to have an average area of circa 4 x 10^3 μm^2, whilst cells on substrates with extra thrombin added were observed to spread ~ 50 % more, resulting in average cell areas of about 6 x 10^3 μm^2. In contrast, the spread area of cells on the fibrin/PIC composite gels was significantly reduced. More cells remained round whilst the spread cells had a smaller area, resulting in an average cell area of about half of cells on fibrin (circa 2 x 10^3 μm^2). One possible explanation is that cell spreading on fibrin/PIC networks may be restricted because of a limited number of accessible adhesion sites. However, since the hMSCs do spread on the lowest fibrin concentration (1 mg/mL), it is unlikely that the number of available adhesion sites is limiting the spreading in all fibrin/PIC samples (with fibrin concentrations up to 5 mg/mL). It was observed that the hMSC surface area was only weakly dependent on the fibrin concentration. The differences in cell area between the different fibrin networks are much more pronounced.

The differentiation of hMSCs into osteoblasts and adipocytes was also studied on the different gels (Figure 4). hMSCs were seeded on the 2 and 4 mg mL^{-1} fibrin samples of the three types of gels. After culturing in mixed adipogenic/osteogenic medium for 10 days, approximately 15 % of the cells had developed into mature adipocytes, as indicated by the Oil Red O staining, independently of the gel type. Differentiation into osteoblasts after culturing for 7 days was similar for both pure fibrin gels and fibrin + extra thrombin gels with ~25 % of the cells staining positive for alkaline phosphatase. In contrast, the presence of PIC in the fibrin gels reduced the differentiation into osteoblasts to only 10 % of the cells.

Discussion

As discussed in the introduction, both bulk and local substrate properties can direct cell behavior.[1-5] It is therefore interesting to disentangle at what scale matrix mechanics is dominating cell spreading and differentiation in our system. As described above, turbidimetry revealed that the fiber architecture is affected by the presence of PIC and by the addition of extra thrombin to fibrin gels. Bulk rheology measurements showed that the presence of PIC affected the mechanics, whilst the addition of extra thrombin had little effect on both the G_0 and the σ_c of the gels.

In the experiments described above, differentiation was only affected by the presence of PIC in the fibrin gels. As the plateau modulus of the composite gels is higher than that of the other gels, one may have expected that more cells differentiate into osteoblasts.[31] This was however not observed, indicating that (bulk) mechanical properties are not the only responsible factor. On the other hand, we observed that the hMSCs spread less on fibrin/PIC substrates. Since cell morphology has also been linked to differentiation,[32] it is possible that the limited cell spreading on the 2D fibrin/PIC substrates is preventing the hMSCs to differentiate into osteoblasts. Because the addition of thrombin does affect cell spreading, the bulk rheology alone cannot explain the differences in cell area. The observed trend in the turbidity measurements corresponds to the cell spreading results. On the networks with the largest fiber diameter, the lowest fiber density, and thus the softest bundles

(the fibrin/PIC composite) the cells have the smallest average area. The opposite is also true; on the networks with the smallest fiber diameter, the highest fiber density and thus the stiffest bundles (in the fibrin gels with extra thrombin) the average cell area is largest. This strongly suggests that cell spreading is influenced by individual fiber architecture and mechanics, rather than by the material's bulk mechanics. It should be noted that the cells were cultured in a 2D environment, in which cell behavior is not necessarily identical to a 3D environment.[33]

In conclusion, two different approaches to modify the structure and mechanics of fibrin gels have been demonstrated. The addition of extra thrombin during gelation increased the density of fibrin fibers but had little effect on the macroscopic mechanics of the fibrin gels. On the other hand, the formation of the fibrin network in the presence of a PIC network resulted in less dense fibrin fibers and a modified macroscopic strain-stiffening response, due to the composite nature of the gel. The overall concentration of fibrin in the gels resulted in a general trend in fiber density and gel stiffness: fibers in standard fibrin gels decreased slightly in diameter and the gels showed increasing stiffness with increasing concentration. The addition of extra thrombin resulted in fibers with strongly increased densities with increasing fibrin concentrations but bulk mechanical properties that matched those of standard fibrin gels. For the fibrin/PIC composite networks little variation in fiber diameters and densities with increasing fibrin concentration was observed, whilst the mechanical properties of the composite gel changed from predominantly PIC-like to predominantly fibrin-like. These series of materials give insight into the effect of the gel morphology and mechanics on hMSC spreading and differentiation. It was found that the average cell area was largest on the bundles with the highest fiber density (fibrin + extra thrombin) and smallest for cells cultured on fibers with the lowest fiber density and thus, presumably, the softest bundles (the fibrin/PIC composite). Since the addition of extra thrombin did not alter the macroscopic strain stiffening response of the gels, the bulk mechanics alone cannot account for the observations. Together with the observation that there was very little variation in cell behavior within a series of gels of increasing fibrin concentration, we conclude that the mechanical properties of individual fibers within these gels likely play an essential

role. Future cell studies should therefore take into account both the macroscopic mechanics of the substrate and the role of microscopic properties of the individual fibers.

Materials and Methods

Gel preparation: Fibrin-only gels were prepared by mixing fibrinogen (from bovine plasma; Sigma Aldrich) solutions in PBS with equal volumes of DMEM-Hepes (Gibco) + 10 % FBS (Gibco) + pen/strep to obtain solutions of 1, 2, 3, 4 and 5 mg mL^{-1}. Gels were obtained after 1 h incubation at 37 °C. In the series with extra thrombin, thrombin (bovine, Sigma Aldrich) was added directly before incubation at 37 °C at a final concentration of 0.5 U mL^{-1}. For the fibrin/PIC composite networks, 2 mg mL^{-1} PIC (synthesized as reported previously[15, 34]) was dissolved in DMEM-Hepes + 10 % FBS + pen/strep by stirring at 4 ^{o}C for at least 24 hours before mixing with the fibrinogen solution.

Turbidimetry: The protocol was adapted from previous work.[18] For a suspension of cylindrical fibers with diameter d, the turbidity t is: $t\lambda^5 = A\mu(\lambda^2 - Br^2)$, with $t = D\ln(10)$, $A = (88/15)c\pi^3 n_s (dn/dc)^2 (1/N_A)$ and $B = (184/231)\pi^2 n_s^2$. Here, D is the optical density, n_s is the refractive index of the solvent, dn/dc is the specific refractive index increment (dn/dc = 0.17594 $cm^3\ g^{-1}$ for fibrin[23]), N_A is Avogadro's number, μ is the mass/length ratio of the fiber, r is the fiber radius and c is the fibrin concentration. From plotting $t\lambda^5$ versus λ^2 and fitting a linear function, the average fiber diameter $d = 2r$ can be obtained. The number of protofibrils per fiber N is calculated from μ through $N = \mu/\mu_0$, where μ_0 = 1.44 x 10^{11} Da cm^{-1} is the mass/length ratio of the protofibril.[35] The fiber density is calculated as $\mu(\pi r^2)^{-1}$ with the assumption that the fibers have a cylindrical shape.[17] For these turbidity measurements, pre-gel solutions were transferred into cuvettes (1 cm path length) and incubated at 37 °C for a minumum of 1.5 h. For turbidimetry analysis, the samples were placed in a Lambda 35 spectrophotometer (Perkin Elmer), with the temperature set at 37 °C. Turbidity data in the wavelength range of 500–800 nm was analyzed using custom-written MATLAB scripts.[18] For the fibrin/PIC samples, the measurement for a 1 mg mL^{-1} PIC hydrogel (which has a much lower optical

density than the fibrin gels) was subtracted as background so the PIC does not contribute to the scattering data.

Rheology: Measurements were performed on a stress-controlled rheometer (Discovery HR-1, TA instruments) in an aluminium parallel-plate geometry with a 40 mm diameter and a 500 µm gap.[36] The samples were loaded into the rheometer in the liquid state at 5 ^{o}C and subsequently heated to 37 ^{o}C. To follow the formation of the fibrin network, the complex modulus G^* was measured by applying an oscillatory deformation with an amplitude of γ = 0.01 and a frequency of ω = 1.0 Hz for 1 hour, after which the storage modulus G' was constant. Drying of the sample was prevented by maintaining a humid atmosphere. The nonlinear stiffening regime was studied at T = 37 ^{o}C using a pre-stress protocol where the material was subjected to a constant pre-stress σ_0 = 0.1 – 800 Pa with a small oscillatory stress superposed at a frequency of ω = 10 – 0.1 Hz. The differential modulus K' was independent of frequency. The oscillatory stress was at least 10 times smaller than the applied pre-stress.

Cell culture and staining: Bone marrow-derived human mesenchymal stem cells (Lonza) were cultured to passage 6 and seeded onto the gels at 1,250 cells cm^{-2} for morphological studies, 2,500 cells cm^{-2} for osteogenic differentiation and 25,000 cells cm^{-2} for adipogenic differentiation in a 1:1 mixture of osteogenic and adipogenic induction medium (DMEM + 10 % FBS + pen/strep, containing 5 x 10^{-7} M dexamethasone, 5 mM β-glycerolphosphate, 0.1 mM ascorbic acid-2-phosphate, 250 µM 3-isobutyl-1-methylxanthine, 5 mg mL^{-1} insulin (from bovine pancreas) and 5 x 10^{-8} M rosiglitazone maleate). After 24 h in culture, cells were fixed and stained with DAPI to detect nuclei and TRITC-phalloidin (Millipore) to stain actin filaments for morphology studies. Significance of differences in cell area were tested using by one-way analysis of variance (ANOVA) with Bonferroni *post hoc* correction. Staining for alkaline phosphatase (as osteogenic marker) and oil red O (as adipogenic marker) was performed after 7 d and 10 d respectively. The fibrin network was labelled with FITC (Sigma Aldrich).

Microscopy: Confocal laser scanning microscopy was performed on a SP2 AOBS from Leica-microsystems using excitation lines 405 nm, 488 nm and 561 nm. All images shown are single optical sections. Contrast and brightness of images were enhanced in order to ease visualization of gel structure and cell morphology. Cell differentiation was analyzed by brightfield microscopy on a Zeiss Axiovert 135 TV which was equipped with a Coolsnap 5M color camera. Images of Oil red O staining underwent a non-linear adjustment to normalize the background color between the different gel types. No processing was applied to the images showing alkaline phosphatase staining.

Acknowledgements

We thank Dr. Aigars Piruska for writing FIJI scripts for morphology analysis and Zaskia Eksteen-Akeroyd for preliminary experiments. Dr. Elisabeth Pierson and Dr. Jurjen Tel are acknowledged for helpful discussions. The department of General Instruments of the Radboud University Nijmegen is acknowledged for providing light microscopy services. We thank the Netherlands Organization for Scientific Research (NWO, VICI Grant 700.10.44 (W.T.S.H.)), the Foundation for Fundamental Research on Matter (FOM), which is financially supported by NWO (G.H.K.), the Dutch Ministry of Education, Culture and Science (Gravity program 024.001.035), the European Commission (Marie Curie IIF Fellowship (N.A.K.)) and Radboud University, Nijmegen for financial support.

References

1. Rozario T, DeSimone DW. The extracellular matrix in development and morphogenesis: A dynamic view. Dev Biol 2010; 341:126-40.

2. Parsons JT, Horwitz AR, Schwartz MA. Cell adhesion: integrating cytoskeletal dynamics and cellular tension. Nature Reviews Molecular Cell Biology 2010; 11:633-43.

3. Engler AJ, Sen S, Sweeney HL, Discher DE. Matrix elasticity directs stem cell lineage specification. Cell 2006; 126:677-89.

4. Trappmann B, Gautrot JE, Connelly JT, Strange DGT, Li Y, Oyen ML, Stuart MAC, Boehm H, Li BJ, Vogel V, et al. Extracellular-matrix tethering regulates stem-cell fate. Nat Mater 2012; 11:642-9.

5. Yang C, Tibbitt MW, Basta L, Anseth KS. Mechanical memory and dosing influence stem cell fate. Nat Mater 2014; 13:645-52.

6. Buehler MJ, Yung YC. Deformation and failure of protein materials in physiologically extreme conditions and disease. Nat Mater 2009; 8:175-88.

7. Storm C, Pastore JJ, MacKintosh FC, Lubensky TC, Janmey PA. Nonlinear elasticity in biological gels. Nature 2005; 435:191-4.

8. Janmey PA, Weitz DA. Dealing with mechanics: mechanisms of force transduction in cells. Trends BiochemSci 2004; 29:364-70.

9. Bausch AR, Kroy K. A bottom-up approach to cell mechanics. Nat Phys 2006; 2:231-8.

10. Discher DE, Janmey P, Wang YL. Tissue cells feel and respond to the stiffness of their substrate. Science 2005; 310:1139-43.

11. Winer JP, Oake S, Janmey PA. Non-linear elasticity of extracellular matrices enables contractile cells to communicate local position and orientation. PLoS One 2009; 4:11.

12. Baker BM, Trappmann B, Wang WY, Sakar MS, Kim IL, Shenoy VB, Burdick JA, Chen CS. Cell-mediated fibre recruitment drives extracellular matrix mechanosensing in engineered fibrillar microenvironments. Nat Mater 2015; advance online publication.

13. Janmey PA, Winer JP, Weisel JW. Fibrin gels and their clinical and bioengineering applications. Journal of the Royal Society Interface 2009; 6:1-10.

14. Kouwer PHJ, Koepf M, Le Sage VAA, Jaspers M, van Buul AM, Eksteen-Akeroyd ZH, Woltinge T, Schwartz E, Kitto HJ, Hoogenboom R, et al. Responsive biomimetic networks from polyisocyanopeptide hydrogels. Nature 2013; 493:651-5.

15. Jaspers M, Dennison M, Mabesoone MFJ, MacKintosh FC, Rowan AE, Kouwer PHJ. Ultra-responsive soft matter from strain-stiffening hydrogels. Nat Commun 2014; 5.

16. Carr ME, Shen LL, Hermans J. Mass-length ratio of fibrin fibers from gel-permeation and light-scattering. Biopolymers 1977; 16:1-15.

17. Carr ME, Hermans J. Size and density of fibrin fibers from turbidity. Macromolecules 1978; 11:46-50.

18. Kurniawan NA, Grimbergen J, Koopman J, Koenderink GH. Factor XIII stiffens fibrin clots by causing fiber compaction. J Thromb Haemost 2014; 12:1687-96.

19. Piechocka IK, Bacabac RG, Potters M, MacKintosh FC, Koenderink GH. Structural hierarchy governs fibrin gel mechanics. Biophys J 2010; 98:2281-9.

20. Piechocka IK, Jansen KA, Broedersz CP, Kurniawan NA, MacKintosh FC, Koenderink GH. Multi-scale strain-stiffening of semiflexible bundle networks. Soft Matter 2016.

21. The PIC bundles are not observed in confocal or turbidity measurements due to the very small bundle diameter of several nanometers.

22. Yang Z, Mochalkin I, Doolittle RF. A model of fibrin formation based on crystal structures of fibrinogen and fibrin fragments complexed with synthetic peptides. Proc Natl Acad Sci U S A 2000; 97:14156-61.

23. Yeromonahos C, Polack B, Caton F. Nanostructure of the fibrin clot. Biophys J 2010; 99:2018-27.

24. Broedersz CP, Kasza KE, Jawerth LM, Munster S, Weitz DA, MacKintosh FC. Measurement of nonlinear rheology of cross-linked biopolymer gels. Soft Matter 2010; 6:4120-7.

25. Bustamante C, Marko JF, Siggia ED, Smith S. Entropic elasticity of lambda-phage DNA. Science 1994; 265:1599-600.

26. Gardel ML, Shin JH, MacKintosh FC, Mahadevan L, Matsudaira P, Weitz DA. Elastic behavior of cross-linked and bundled actin networks. Science 2004; 304:1301-5.

27. Mackintosh FC, Kas J, Janmey PA. Elasticity of semiflexible biopolymer networks. Phys Rev Lett 1995; 75:4425-8.

28. From calculations based on a semi flexible network model we found that the increase in *N* upon adding extra thrombin cannot be compensated by an increase in the pore size of the network. Therefore, the transition to a loose fiber regime must account for the constant plateau modulus.

29. Bathe M, Heussinger C, Claessens M, Bausch AR, Frey E. Cytoskeletal bundle mechanics. Biophys J 2008; 94:2955-64.

30. Trappmann B, Chen CS. How cells sense extracellular matrix stiffness: a material's perspective. Curr Opin Biotechnol 2013; 24:948-53.

31. Zhao W, Li XW, Liu XY, Zhang N, Wen XJ. Effects of substrate stiffness on adipogenic and osteogenic differentiation of human mesenchymal stem cells. Materials Science & Engineering C-Materials for Biological Applications 2014; 40:316-23.

32. McBeath R, Pirone DM, Nelson CM, Bhadriraju K, Chen CS. Cell shape, cytoskeletal tension, and RhoA regulate stem cell lineage commitment. Dev Cell 2004; 6:483-95.

33. Baker BM, Chen CS. Deconstructing the third dimension - how 3D culture microenvironments alter cellular cues. J Cell Sci 2012; 125:3015-24.

34. Koepf M, Kitto HJ, Schwartz E, Kouwer PHJ, Nolte RJM, Rowan AE. Preparation and characterization of non-linear poly(ethylene glycol) analogs from oligo(ethylene glycol) functionalized polyisocyanopeptides. Eur Polym J 2013; 49:1510-22.

35. De Spirito M, Arcovito G, Papi M, Rocco M, Ferri F. Small- and wide-angle elastic light scattering study of fibrin structure. Journal of Applied Crystallography 2003; 36:636-41.

36. Because of the variable temperature program and the large negative normal stresses in semi-flexible polymer networks, we use the plate-plate geometry by default. Test measurements with isothermal cone-plate and large volume Couette geometries give identical mechanical results, both in the linear and the nonlinear regime.

Figure legends

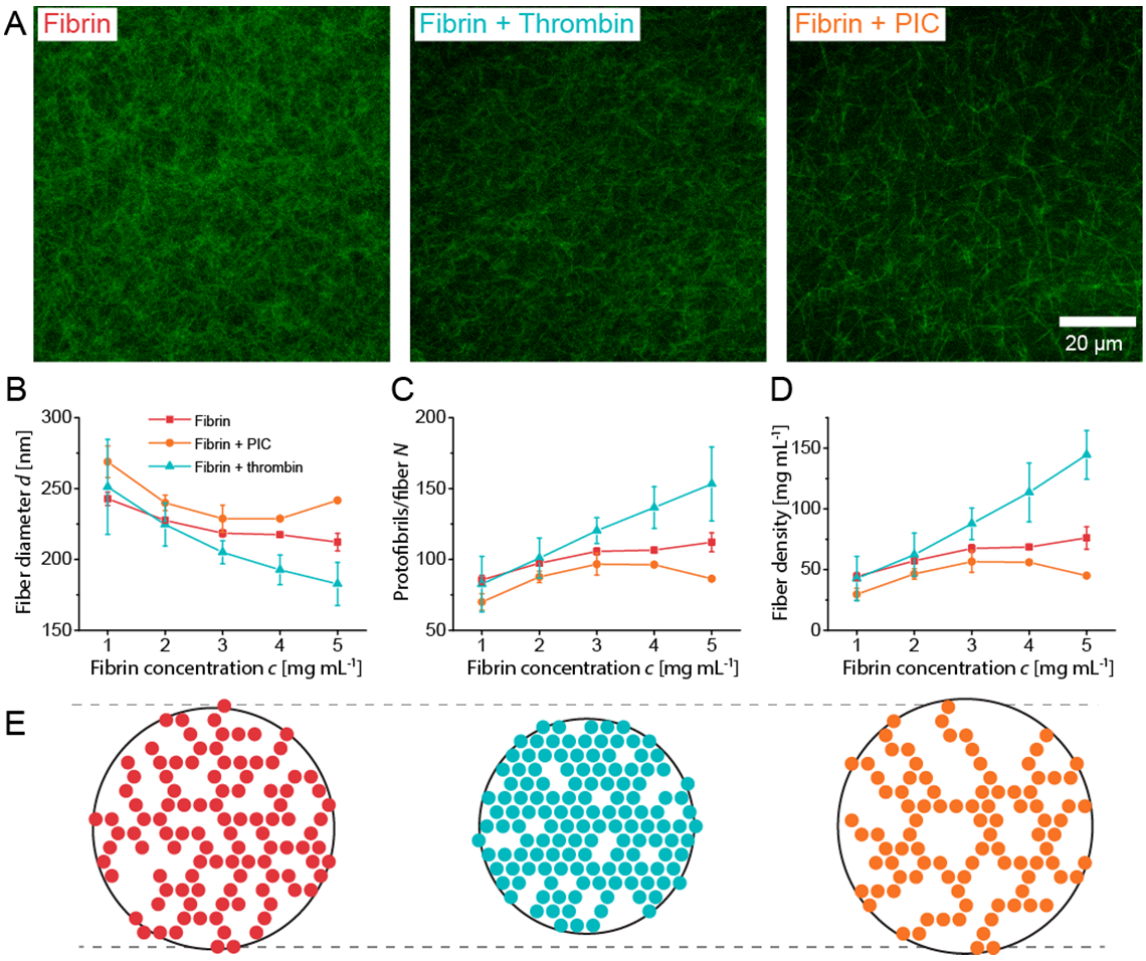

Figure 1: Tuning of the architecture of the fibrin network by addition of extra thrombin or PIC during gel preparation. A) Confocal images show that the presence of PIC results in slightly thicker bundles. B) Turbidity experiments quantified the fiber diameter. C) The number of protofibrils per fiber was obtained from turbidity measurements, showing that the addition of thrombin results in the highest number of protofibrils per fiber and the addition of PIC in the lowest. D) The protein mass density within the fibers was calculated from the fiber diameter and protofibrils/fiber showing that PIC decreases the fiber density and the addition of extra thrombin results in the densest fibers. E) Schematic representations of fiber cross-section showing a model how the differences in fiber density may arise.

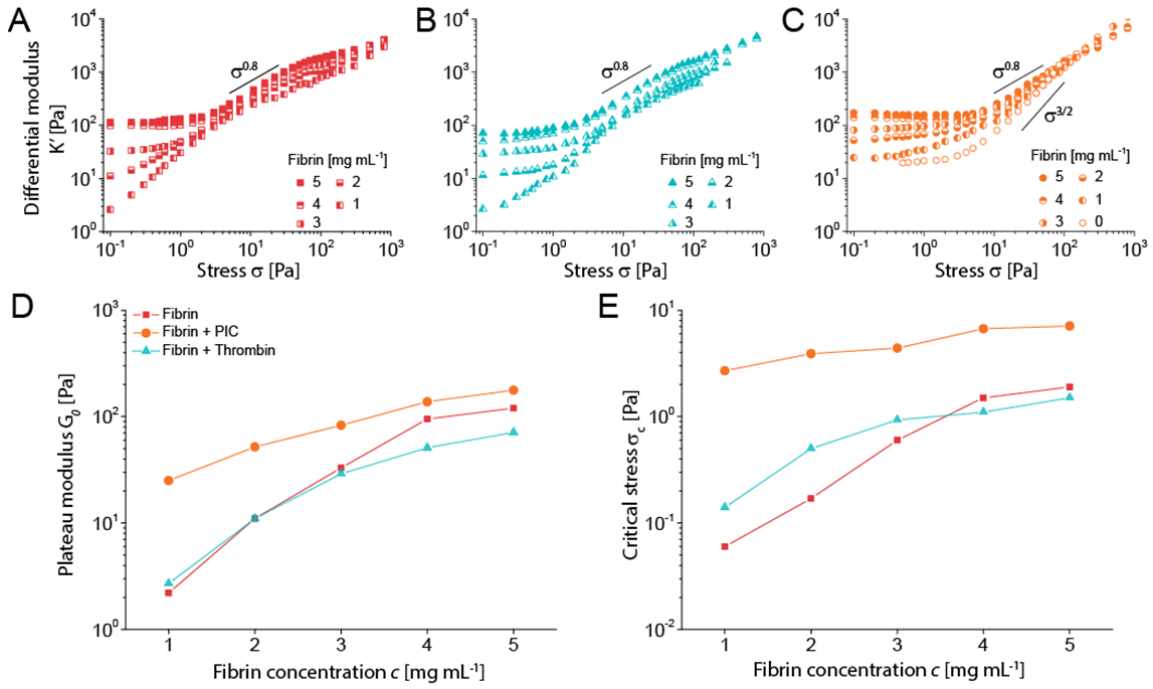

Figure 2: The differential modulus *K'* as a function of stress for A) fibrin gels, B) fibrin gels with extra thrombin added and C) fibrin/PIC composite gels. D) The plateau modulus G_0 and E) The critical stress σ_c of these gels as a function of fibrin concentration.

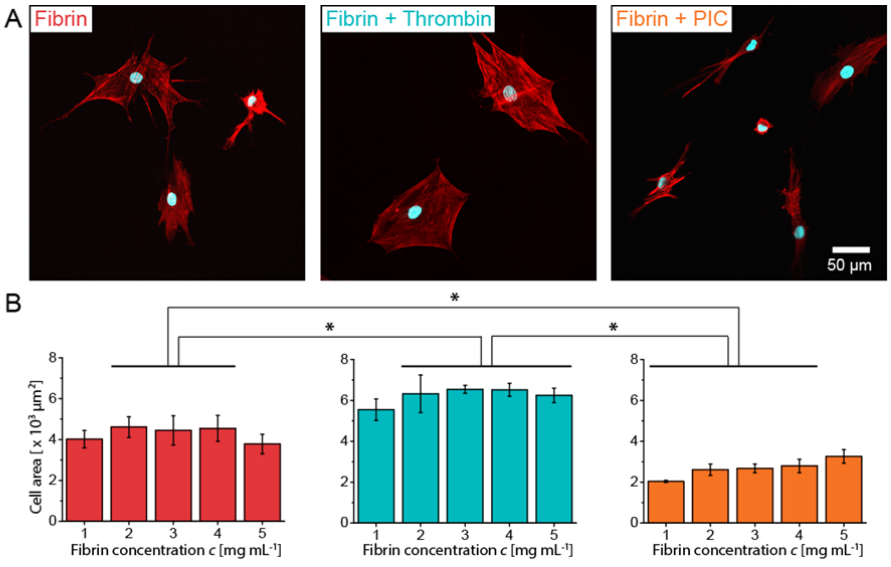

Figure 3: hMSC spreading is affected by the structure and mechanical properties of the fibrin network. Fibrin gels that were formed with extra thrombin stimulate the cells to spread more in comparison to pure fibrin. In contrast, the addition of PIC to fibrin substrates reduces hMSC spreading. A) Confocal images of hMSCs after 24 h culture on 2 mg mL^{-1} fibrin gels showing F-actin (phalloidin staining; red) and nucleus (DAPI staining; cyan). B)

Quantification of cell spreading 24 h after seeding on the fibrin, fibrin + thrombin and fibrin/PIC gels. Mean ± s.d. * $P < 0.05$

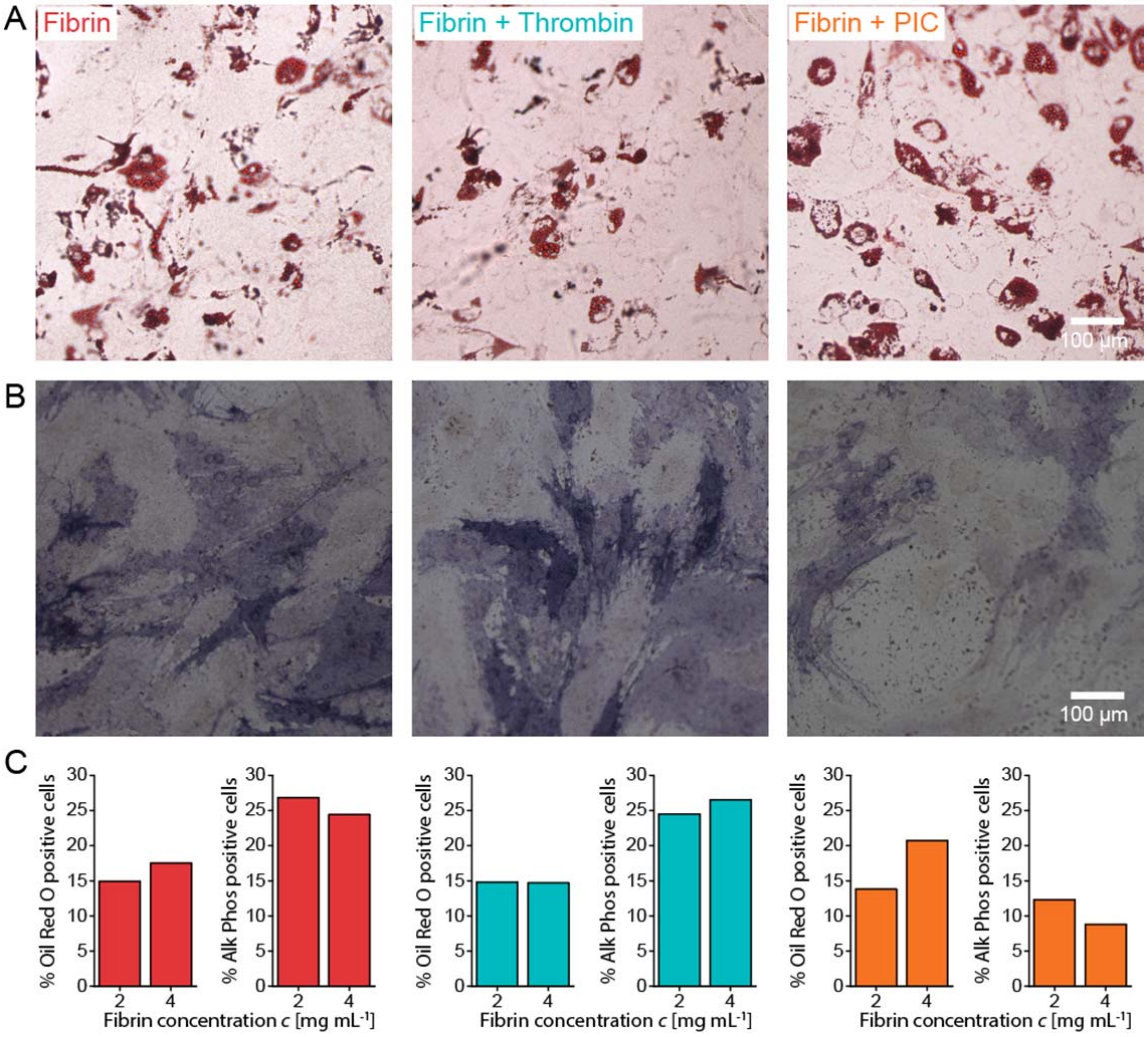

Figure 4: The influence of the fibrin structure on differentiation of hMSCs. A) Oil Red O and B) alkaline phosphatase staining on the fibrin, fibrin + thrombin and fibrin/PIC gels. C) Quantification of differentiation after 7 d (Alk Phos) and 10 d (Oil Red O) in culture.